Science of the Total Environment 744 (2020) 140837

Contents lists available at ScienceDirect

Science of the Total Environment

journal homepage: www.elsevier.com/locate/scitotenv

Meteorological influences on $PM_{2.5}$ and O_3 trends and associated health burden since China's clean air actions

Lei Chen [a,b], Jia Zhu [a], Hong Liao [a,*], Yang Yang [a], Xu Yue [a]

[a] Jiangsu Key Laboratory of Atmospheric Environment Monitoring and Pollution Control, Jiangsu Collaborative Innovation Center of Atmospheric Environment and Equipment Technology, School of Environmental Science and Engineering, Nanjing University of Information Science & Technology, Nanjing 210044, China
[b] Key Laboratory of Meteorological Disaster, Ministry of Education (KLME), Joint International Research Laboratory of Climate and Environment Change (ILCEC), Collaborative Innovation Center on Forecast and Evaluation of Meteorological Disasters (CIC-FEMD), Nanjing University of Information Science & Technology, Nanjing 210044, China

HIGHLIGHTS

- The meteorology-driven $PM_{2.5}$ (O_3) trends were −0.5 ~ −2.0 (+0.7 ~ +0.8) μg m^{-3} yr^{-1}.
- The decreased relative humidity explained 55% of meteorology-driven $PM_{2.5}$ trend.
- The increased boundary layer height explained 42% of meteorology-driven O_3 trend.
- The meteorology contributed 10– 26% of the decreasing trends in $PM_{2.5}$-related deaths.
- The meteorology contributed 15– 31% of the increasing trends in O_3-related deaths.

GRAPHICAL ABSTRACT

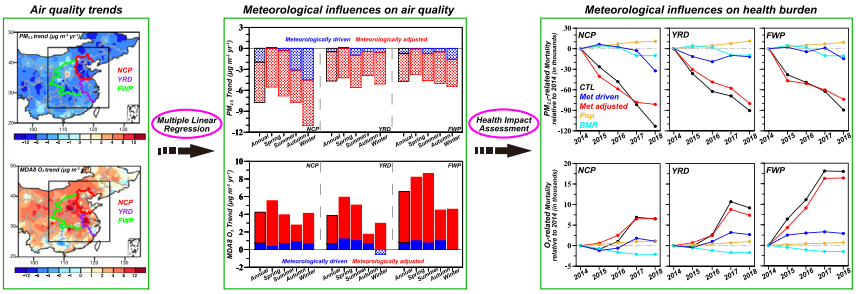

ARTICLE INFO

Article history:
Received 14 May 2020
Received in revised form 3 July 2020
Accepted 7 July 2020
Available online 13 July 2020

Editor: Jianmin Chen

Keywords:
$PM_{2.5}$
Ozone
Meteorological influence
Health impact

ABSTRACT

Stringent clean air actions have been implemented to improve air quality in China since 2013. In addition to anthropogenic emission abatements, the changes in air quality may be modulated also by meteorology. In this study, we developed multiple linear regression models to quantify meteorological influences on the trends in fine particulate matter ($PM_{2.5}$) and ozone (O_3) concentrations and associated health burden over three polluted regions of China, i.e., North China Plain, Yangtze River Delta, and Fen-wei Plain during 2014–2018, with a novel focus on the contributions of the most influential meteorological factors to $PM_{2.5}$ and O_3 trends as well as the meteorological contributions to $PM_{2.5}$- and O_3-related mortality trends. The meteorology-driven $PM_{2.5}$ (O_3) trends for the three regions were −0.5~−2.0 (+0.7~+0.8) μg m^{-3} yr^{-1}, contributing 10– 26% (12– 18%) of the observed five-year decreasing $PM_{2.5}$ (increasing O_3) trends. The decreased relative humidity (increased daytime planetary boundary layer height) was identified to be the most influential meteorological factor and explained 55% (42%) of the largest meteorology-driven $PM_{2.5}$ (O_3) trend among all regions and seasons. The meteorology-driven decreases in $PM_{2.5}$ (increases in O_3) concentrations led to overall decreases in $PM_{2.5}$-related (increases in O_3-related) mortalities with trends of −2.2~−7.4 (+0.5~+0.9) thousand yr^{-1} for the three regions, accounting for 10– 26% (15– 31%) of the total decreasing (increasing) trends in $PM_{2.5}$-related (O_3-related) mortalities. The results emphasize the important role of meteorology in $PM_{2.5}$ and O_3 air quality and associated health burden over China, and have important implications for China's air quality planning. In particular, more efforts in emission control should be taken to offset the adverse effects on ozone caused by meteorology.

* Corresponding author at: Nanjing University of Information Science & Technology, No.219, Ningliu Road, Nanjing, Jiangsu, China.
E-mail address: hongliao@nuist.edu.cn (H. Liao).

https://doi.org/10.1016/j.scitotenv.2020.140837
0048-9697/

1. Introduction

Air pollution has become a serious environmental problem during recent years in China, and has aroused unprecedented public concerns. Epidemiologists have confirmed associations between air pollutants and health burden (Lelieveld et al., 2015; Silva et al., 2017; Nieuwenhuijsen et al., 2018). Therefore, a series of stringent clean air actions have been implemented to improve air quality in China since 2013 (State Council of the People's Republic of China, 2013, 2018). As a result, air quality index averaged over China has decreased 16% over 2014–2018 (Fan et al., 2020). However, the improvements in air quality owing to anthropogenic emission abatements may be modulated by meteorology (Jacob and Winner, 2009). The meteorology may further contribute to changes in air quality-attributed premature mortality. Understanding the extent to which the changed meteorology can affect strategies to improve air quality and health effect is an important aspect of this adaptation. Therefore, it is fundamental to assess the impacts of meteorological variation on air quality and associated health burden since China's clean air actions.

Fine particulate matter with an aerodynamic diameter of 2.5 μm or less ($PM_{2.5}$) and ozone (O_3) are the two air pollutants of most concern for public health. Both $PM_{2.5}$ and O_3 concentrations can be largely influenced by anthropogenic emissions. The $PM_{2.5}$ levels are affected by the anthropogenic emissions of sulfur dioxide (SO_2), nitrogen oxides (NO_x), ammonia (NH_3), black carbon (BC), organic carbon (OC), and non-methane volatile organic compounds (NMVOCs), while the dominant source of surface O_3 is the photochemical oxidation of carbon monoxide (CO), methane (CH_4), and NMVOCs in the presence of NO_x (Zhu and Liao, 2016; Yue et al., 2017). The responses of $PM_{2.5}$ and O_3 to variations in anthropogenic emissions have been widely investigated (Querol et al., 2014; Lou et al., 2015; Gao et al., 2016; Tao et al., 2020). Generally, positive effects of reduced emissions are confirmed for $PM_{2.5}$ (i.e., improved $PM_{2.5}$ air quality) since 2013 (Zhang et al., 2019a), while the impacts on O_3 vary by region and time because of the nonlinear relationship between O_3 and its precursors (Ding et al., 2019a).

Strong sensitivities of $PM_{2.5}$ and O_3 air quality to meteorology can be understood via changes in physical and chemical processes (Zhang et al., 2010; Han et al., 2014; Huang et al., 2018b; Zhang et al., 2018a). A decreasing trend of wind resource is unfavorable for air pollution dispersion (Yang et al., 2017; Zhang and Wang, 2020). The decreased planetary boundary layer height (PBLH) may restrain vertical mixing and lead to the accumulation of particles (Gao et al., 2015; Chen et al., 2019a). An increase in temperature or solar radiation can enhance chemical reaction rates of O_3 (Unger et al., 2006; Lee et al., 2014). Less precipitation, which means weaker wet removal process, may increase air pollutant concentrations (Racherla and Adams, 2006; Wang et al., 2018).

Numerical simulations or statistical methods have been applied to assess meteorological influences on $PM_{2.5}$ and O_3 trends in China by several studies (Zhu et al., 2012; Ma et al., 2016; Han et al., 2020). By using WRF-Chem model, Gao et al. (2020) designed a numerical experiment with fixed anthropogenic emissions, and reported an increasing trend of 2.1 $\mu g\ m^{-3}\ yr^{-1}$ for wintertime $PM_{2.5}$ in Beijing in response to variations in meteorological conditions over 2002–2016. Applying a stepwise multiple linear regression (MLR) model, Zhai et al. (2019) calculated the meteorology-driven $PM_{2.5}$ trend to be -1.3 $\mu g\ m^{-3}\ yr^{-1}$ in Beijing-Tianjin-Hebei during 2013–2018. Based on the simulation results from WRF-CMAQ, Liu and Wang (2020) found that meteorological influences on O_3 trends in China over 2013–2017 varied by regions, and the variations in maximum daily 8-hour average ozone (MDA8 O_3) due to changed meteorology ranged from -12.7 to $+15.3$ ppb over China for years 2014–2017 relative to 2013. Han et al. (2020) used a MLR method and revealed that meteorology contributed to 18% of the increase in summertime O_3 averaged over eastern China during 2013–2018.

Several recent studies have estimated the temporal variations in $PM_{2.5}$- and O_3-related premature mortality (Zheng et al., 2017; Huang et al., 2018a; Boogaard et al., 2019; Xie et al., 2019). By using the WRF-CMAQ model, Ding et al. (2019b) reported that premature mortality attributable to $PM_{2.5}$ in China was 1.4 million in 2013 but was substantially reduced to 1.1 million in 2017. Based on the simulation results from GEOS-Chem model, Dang and Liao (2019) estimated that premature mortality caused by O_3 exposure increased by 16.0 thousand in 2017 relative to 2012 over eastern China.

Although these existing studies have revealed the total impacts of meteorology on $PM_{2.5}$ and O_3 air quality trends in China, the relative contributions of key meteorological variables to the trends remain unclear. Identifying the most influential meteorological variable and quantifying its contribution will be helpful to comprehensively understand the meteorological effects on variations in air quality. Furthermore, although previous studies have estimated the temporal variations in $PM_{2.5}$- and O_3-attributable excess deaths since 2013, few studies attempt to quantitatively distinguish the individual contribution of each underlying driver to the variations in $PM_{2.5}$- and O_3-related health burden, especially the contribution from meteorological variations.

This study aims to 1) quantify meteorological influences on trends in $PM_{2.5}$ and O_3 concentrations in China over 2014–2018, with a novel focus on the contribution of the most influential meteorological factor to $PM_{2.5}$ and O_3 trends, by developing MLR models which correlate observed $PM_{2.5}$ and O_3 concentrations with meteorological variables during four seasons. 2) estimate the trends in $PM_{2.5}$- and O_3-related premature mortality in China during 2014–2018, and distinguish the respective contributions of underlying driving factors, highlighting the contribution from meteorologically driven variations in $PM_{2.5}$ and O_3 concentrations. We pay special attention to the trends in $PM_{2.5}$ and O_3 air quality and associated health burden over three polluted regions in China, i.e., North China Plain (NCP), Yangtze River Delta (YRD), and Fen-wei Plain (FWP).

2. Data and methods

2.1. Meteorological data

Meteorological parameters for 2014–2018 are retrieved from European Centre for Medium-Range Weather Forecasts Reanalysis Interim (ERA-Interim) data (https://apps.ecmwf.int/datasets/), with the spatial and temporal resolutions of 0.5° × 0.5° and 3-h, respectively. Following Leung et al. (2018) and Li et al. (2019), twenty-six meteorological parameters (Table S1) are adopted as original candidate meteorological predictors for MLR models. We average them over either 24-h or daytime hours (08:00–17:00 local time) to construct the following MLR model.

2.2. Air quality data

Hourly concentrations of observed $PM_{2.5}$ and O_3 for 2014–2018 were obtained from China National Environmental Monitoring Centre (http://106.37.208.233:20035/). The network covers 944 sites in 2014, growing to nearly 1500 sites in 2018. We conduct data quality assurance following Zhu et al. (2019). The daily mean $PM_{2.5}$ concentrations and daily MDA8 O_3 concentrations are calculated to conduct the MLR analysis. In order to generate continuous gridded concentration data, we interpolate all the site concentrations onto the ERA-Interim grid (0.5° × 0.5°), by using inverse distance weighting (IDW) method (Tai et al., 2012; Shen et al., 2017). Detailed descriptions of the IDW method, and the comparison between gridded and site concentrations are shown in Text S1 and Figs. S1–S2. Fig. 1 shows the spatial distributions of 5-year average site and gridded pollutant concentrations. The interpolated results exhibit better performance in denser and more polluted regions, e.g., NCP, YRD, and FWP, where this study is mainly focused on for further analysis.

2.3. Multiple linear regression model and meteorologically driven variation

Multiple linear regression (MLR) model establishes a function between a response variable and several explanatory (predictor) variables.

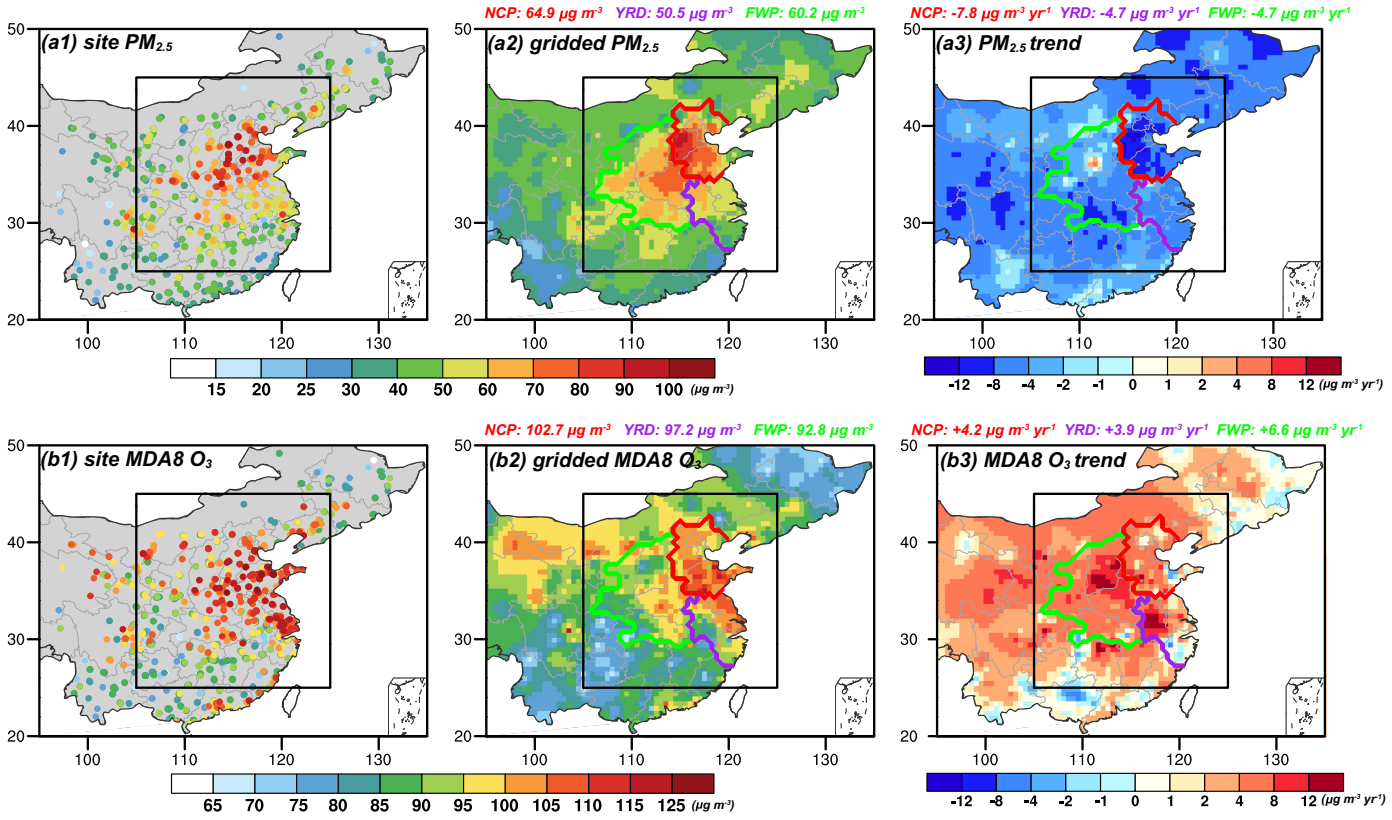

Fig. 1. Spatial distributions of 5-year (2014–2018) average (a1) site $PM_{2.5}$, (b1) site MDA8 O_3, (a2) gridded $PM_{2.5}$, and (b2) gridded MDA8 O_3 concentrations, as well as 5-year trends in gridded (a3) $PM_{2.5}$ and (b3) MDA8 O_3 concentrations over China. The black box covers three polluted regions, i.e. North China Plain (NCP), Yangtze River Delta (YRD), and Fen-wei Plain (FWP), where this study is mainly focused on. The borders of NCP, YRD, and FWP are shown in red, purple, and green, respectively. The calculated gridded concentrations and trends averaged over each region are listed in corresponding colors. (For interpretation of the references to colour in this figure legend, the reader is referred to the web version of this article.)

In order to quantify the meteorological impacts on changes and trends in air quality, we develop a stepwise MLR model in this study to establish relationships between pollutant ($PM_{2.5}$ or MDA8 O_3) concentrations and a set of meteorological variables (predictors) for each region (NCP, YRD, and FWP) and each season (spring, summer, autumn, and winter). The MLR model has been successfully applied to analyze meteorological influences on $PM_{2.5}$ and O_3 variation (Tai et al., 2010; Yang et al., 2019), and takes the following form:

$$C_{i,s,r}(t) = b_{0,i,s,r} + \sum_{k=1}^{N} b_{k,i,s,r} \times Met_k(t) + \varepsilon \quad (1)$$

where $C_{i,s,r}(t)$ is the observed daily concentration of pollutant i ($PM_{2.5}$ or MDA8 O_3) for season s and region r, $Met_k(t)$ is one of the N meteorological predictors, b_0 is the intercept term, b_k is the regression coefficient for the k-th meteorological predictor, and ε is the residual term.

Superior to previous studies, this study conducts more comprehensive selection procedures to obtain "optimal meteorological predictors", shown as the following steps:

Step 1) The correlation coefficients between $PM_{2.5}$ (MDA8 O_3) concentrations and original twenty-six candidate meteorological variables (called "predictors version-0") are calculated across each region in each season during 2014–2018 (Tables S2 and S3). The meteorological variables, which are statistically significant at the 99% confidence level, are retained as candidate predictors (called "predictors version-1") for next selection step.

Step 2) Despite its success in many applications, the MLR model faces serious difficulties when meteorological predictors are correlated with each other. To minimize the influences of correlations between predictors, the variance inflation factor (VIF) is used to test the multicollinearity problem (Altland, 1999; Che et al., 2019). As a measure of collinearity between variables, VIF is calculated as follows:

$$VIF = \frac{1}{1-R_i^2} \quad (2)$$

where R_i^2 is the coefficient of determination obtained by regression between the i-th predictor and other predictors. We set the threshold of 10 for VIF to represent the maximum acceptability of collinearity (Kutner et al., 2004). Therefore, the meteorological variables with VIF larger than 10 are removed, and the remaining candidate variables are retained as "predictors version-2" for next selection step.

Step 3) In order to obtain the best model fit, the regression is done stepwise by adding or removing predictors based on Akaike Information Criterion (AIC) statistics (Akaike, 1969). When AIC reaches the minimum, the "predictors version-3" are obtained. AIC is calculated using the following equation:

$$AIC = T \times \ln\left(\frac{SSE}{T}\right) + 2 \times (k+1) \quad (3)$$

where SSE refers to the sum of squared errors $\sum (C(t) - P(t))^2$, in which $C(t)$ is the observed concentration, and $P(t)$ is the predicted concentration by MLR; T is the number of observations used for estimation; k is the number of predictors used in this regression. After this step, we obtain the "optimal meteorological predictors".

The optimal meteorological variables, calculated intercepts (b_0), regression coefficients (b_k), and adjusted coefficients of determinations (R^2) for each region and each season, are listed in Tables S4 and S5. The calculated adjusted R^2, which estimate the fraction of variability

described by MLR, range from 0.2 to 0.6 for $PM_{2.5}$ and from 0.5 to 0.8 for MDA8 O_3, indicating that the MLR models perform fairly well.

Once the MLR models are established, the meteorologically driven change (or trend) in pollutant concentration (ΔP) can be calculated based on the predicted concentration by MLR ($P(t)$) directly or calculated as:

$$\Delta P_{i,s,r} = \sum_{k=1}^{N} b_{k,i,s,r} \times \Delta Met_k \quad (4)$$

where ΔMet_k represents the change (or trend) in the k-th meteorological variable. The non-meteorologically driven change (or trend), i.e., meteorologically adjusted change (or trend), which is mainly attributed to changes in anthropogenic emissions (Seo et al., 2018; Chen et al., 2020), can be obtained from the difference between observed (ΔC) and meteorologically driven (ΔP) values. Relative contribution of each meteorological variable to the total meteorology-driven change (or trend) is quantified by the ratio of ($b_k \times \Delta Met_k$) to ΔP. The meteorological variable, which makes the largest contribution, is regarded as the most influential meteorological variable for $PM_{2.5}$ (O_3) changes or trends.

2.4. Health impact assessment and meteorologically driven variation

The health impact of air pollution is estimated as premature human mortality using the following equation:

$$\Delta Mort = BMR \times Pop \times AF \quad (5)$$

where $\Delta Mort$ is the excess death due to $PM_{2.5}$ or O_3 exposure, BMR is the baseline mortality rate for a specific disease, Pop is the exposed population (adults ≥25 years old), and AF is the attributable fraction defined as $AF = 1 - 1/RR$. The RR, calculated as concentration-response function (CRF), is the relative risk of cause-specific death attributable to the change in pollutant concentration.

2.4.1. Baseline mortality rate (BMR)

The annual national cause-specific and age-specific baseline mortality rates (BMR) are collected from the Global Burden of Disease study (GBD) results tool (http://ghdx.healthdata.org/gbd-results-tool). We obtain China's BMR data for noncommunicable diseases (NCD), lower respiratory infections (LRI), and chronic respiratory diseases (CRD) from 2014 to 2017. The BMR data in 2018 are unavailable during the conduct of this study and therefore we adopt the BMR data in 2017 as those in 2018.

2.4.2. Population (Pop)

To obtain gridded and age-specific population data in China for years 2014–2018, we use a combination of the provincial population data from the China Statistical Yearbook (http://www.stats.gov.cn/tjsj/ndsj/) and the gridded population data from Global Population for World (GPW) dataset (https://sedac.ciesin.columbia.edu/data/collection/gpw-v4/sets/browse). The provincial age-specific population is available for every year, while the gridded population at the 0.5° × 0.5° resolution is available for every five years (i.e., 2010, 2015, 2020, etc.). We first calculate the proportions of gridded population to provincial population with the gridded and provincial data for year 2015. Assuming the proportions are constant, the gridded and age-specific population for 2014–2018 can be obtained through multiplying the yearly provincial age-specific population (age ≥ 25 years) by the proportions.

2.4.3. Concentration-response function (CRF)

1) For $PM_{2.5}$, RR is derived from the recent Global Exposure Mortality Model (GEMM), which addresses many limitations associated with the widely used Integrated Exposure-Response (IER) model and provides better estimates for highly polluted areas such as China (Burnett et al., 2018; Zhang et al., 2018b). The GEMM estimates $PM_{2.5}$-related mortality due to noncommunicable diseases (NCD) and lower respiratory infections (LRI). The GEMM NCD + LRI takes the following form:

$$RR(C) = exp\left(\frac{\theta \times log\frac{C-C_0}{\alpha}+1}{1+exp\left(-\frac{C-C_0-\mu}{\nu}\right)}\right) \quad (6)$$

for adults older than 25 and ambient $PM_{2.5}$ concentrations (C) larger than C_0 (2.4 μg m^{-3}). Age-specific parameters θ, α, μ, and ν are taken from Burnett et al. (2018) with inclusion of Chinese cohort. Following Silva et al. (2016), we conduct 1000 Monte Carlo simulations that randomly sampled from normal distributions of these parameters to estimate the uncertainty.

2) For O_3, RR is calculated using the CRF from Jerrett et al. (2009) and Anenberg et al. (2010), following Eq. (7):

$$RR(C) = exp^{\beta(C-C_0)} \quad (7)$$

for adults above 25 and ambient O_3 concentrations (C) above C_0. We use the annual mean MDA8 O_3 concentration for C and 26.7 ppb for threshold concentration C_0, as did in Turner et al. (2016) and Malley et al. (2017). β is the concentration response factor, which indicates that a 10-ppb increase in annual mean MDA8 O_3 concentration is associated with a 12% (95% CI, 8– 16%) increase in RR (Turner et al., 2016). In this study, we evaluate O_3-related mortality due to all chronic respiratory diseases (CRD) based on Jerrett et al. (2009). However, we use adults above 25, to be consistent with $PM_{2.5}$-related mortality estimate, following Silva et al. (2016) and Zhang et al. (2018b), even though the estimation from Jerrett et al. (2009) is for adults above 30. The same method as $PM_{2.5}$ is adopted to calculate the uncertainty.

The premature mortality estimation (i.e., Eq. (5)) indicates that the variations in excess deaths are determined by the variations in BMR, Pop, and concentration (Conc). The variations in Conc are further influenced by meteorological variations (meteorologically driven) and non-meteorological variations (meteorologically adjusted), as shown in Section 2.3. To evaluate the individual contribution to the $PM_{2.5}$- and O_3-related mortality variations during 2014–2018 from each driving factor, i.e., variation in meteorologically driven (Met driven) Conc, variation in meteorologically adjusted (Met adjusted) Conc, variation in Pop, and variation in BMR, we perform experiments for five cases in Table 1. Experiment "CTL" represents the normal condition. The mortality variations owing to Conc variation alone (Pop variation alone, BMR variation alone) are quantified by changing the Conc (Pop, BMR) from 2014 to 2018 in experiment "Conc" ("Pop", "BMR"), but keeping the other two factors fixed at 2014 levels. The mortality variations attributed to Conc variation are further decomposed into Met driven mortality variations and Met adjusted mortality variations. The Met driven mortality variations can be obtained based on Met driven Conc variation (Section 2.3) in experiment "Met driven". The Met adjusted mortality variations can be calculated by the difference between those in experiment "Conc" and experiment "Met driven". The relative contribution from each driver is quantified by the ratio of the mortality change owing to each factor alone to the total mortality change from 2014 to 2018. Relative contributions of individual drivers are normalized owing to the nonlinearity of health impacts from different driving factors.

3. Meteorological influences on $PM_{2.5}$ air quality

3.1. Spatiotemporal characteristics of $PM_{2.5}$ concentrations for 2014–2018

Fig. 1(a2) shows the spatial distribution of five-year (2014–2018) average $PM_{2.5}$ concentrations over China. The observed $PM_{2.5}$

Table 1
Experimental design for quantifying the individual contribution from each driving factor to the mortality variations during 2014–2018.

Experiment	Concentration (Conc)	Population (Pop)	Baseline mortality rate (BMR)	Purpose
CTL	2014–2018[a]	2014–2018	2014–2018	Normal condition
Conc	2014–2018[a]	Fixed at 2014 level	Fixed at 2014 level	Examine the mortality variations owing to Conc variation alone
Met driven	2014–2018[b] (Met driven)	Fixed at 2014 level	Fixed at 2014 level	Examine the mortality variations owing to Met driven Conc variation alone
Pop	Fixed at 2014 level	2014–2018	Fixed at 2014 level	Examine the mortality variations owing to Pop variation alone
BMR	Fixed at 2014 level	Fixed at 2014 level	2014–2018	Examine the mortality variations owing to BMR variation alone

[a] The observed concentrations vary from 2014 to 2018 in CTL and Conc experiments.
[b] The concentrations vary from 2014 to 2018 driven by meteorological variations alone in Met driven experiment.

concentrations exhibited high values in NCP, YRD, and FWP, three regions this study was focused on. The five-year mean $PM_{2.5}$ concentrations averaged over NCP, YRD, and FWP were calculated to be 64.9 μg m^{-3}, 50.5 μg m^{-3}, and 60.2 μg m^{-3} respectively, all of which were much higher than the National Ambient Air Quality Standards (i.e., 35 μg m^{-3}). Fig. 1(a3) exhibits the spatial distribution of five-year trends in observed $PM_{2.5}$ concentrations over China. There were general decreasing trends across all of China, with average trends of −7.8 μg m^{-3} yr^{-1}, −4.7 μg m^{-3} yr^{-1}, and − 4.7 μg m^{-3} yr^{-1} for NCP, YRD, and FWP. Yearly $PM_{2.5}$ levels over 2014–2018 for the three regions are presented in Fig. 2(a). Significant decreases were observed in NCP, YRD, and FWP, with reductions of 32.2 μg m^{-3} (39%), 20.6 μg m^{-3} (33%), and 21.9 μg m^{-3} (30%), respectively, from 2014 to 2018. The decreased anthropogenic emissions of SO_2, NO_x, BC, OC, and primary $PM_{2.5}$ (shown in Fig. S3) were regarded as the main causes of improved $PM_{2.5}$ air quality (Zhang et al., 2019a). In this study, the $PM_{2.5}$ decreases from 2014 to 2018 due to non-meteorological variations (i.e., "meteorologically adjusted"), reasonably attributed to reduced anthropogenic emissions, were estimated to be 23.5 μg m^{-3}, 18.0 μg m^{-3}, and

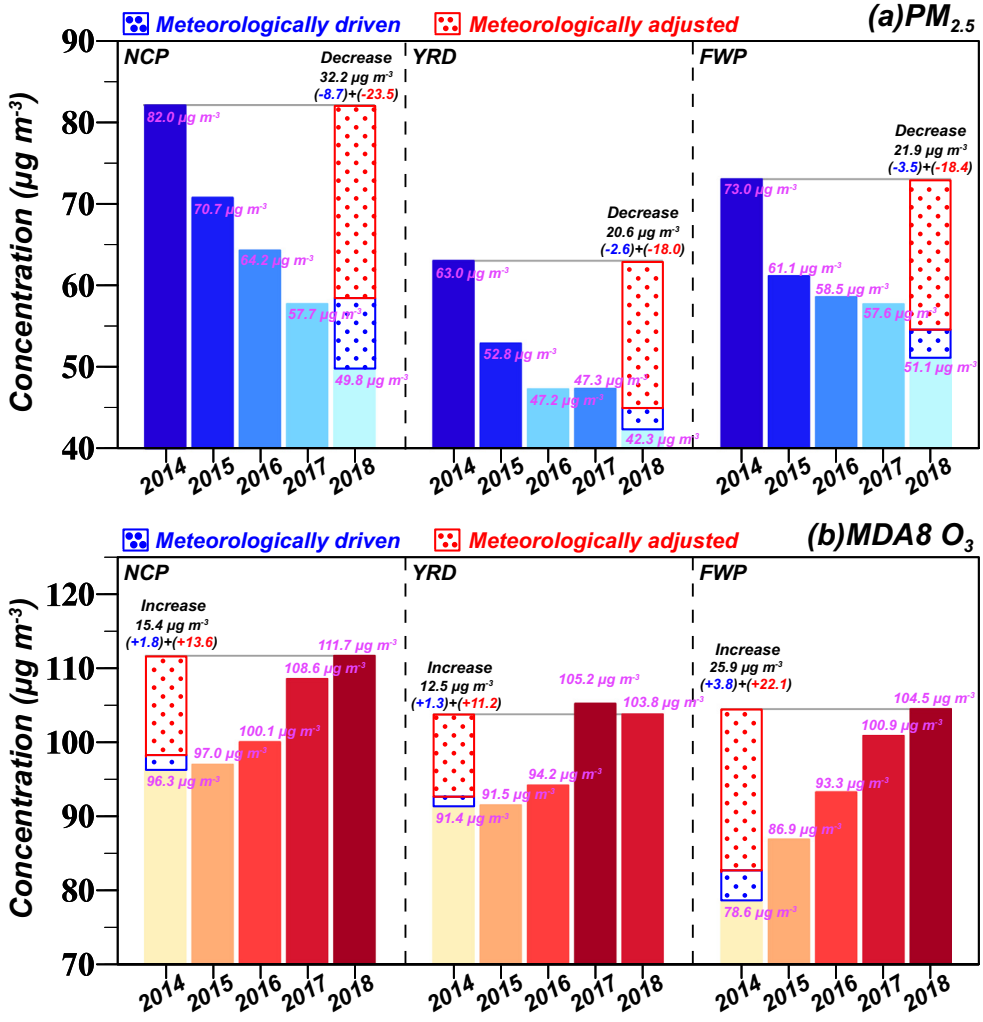

Fig. 2. Observed, meteorologically driven, and meteorologically adjusted changes in (a) $PM_{2.5}$ and (b) MDA8 O_3 concentrations from 2014 to 2018 for NCP, YRD, and FWP. Observed annual mean $PM_{2.5}$ and MDA8 O_3 concentrations for 2014–2018 are shown in solid bars and purple numbers. Black values represent observed $PM_{2.5}$ decreases and MDA8 O_3 increases from 2014 to 2018. Blue dotted bars and values represent meteorologically driven changes in $PM_{2.5}$ or MDA8 O_3 concentrations from 2014 to 2018, while those in red represent non-meteorological (i.e., meteorologically adjusted) changes reasonably attributed to changed anthropogenic emissions. (For interpretation of the references to colour in this figure legend, the reader is referred to the web version of this article.)

18.4 μg m^{-3} for NCP, YRD, and FWP, accounting for 73%, 87%, and 84%, respectively, of observed $PM_{2.5}$ decreases (Fig. 2(a)). Similar contributions were reported in other studies (Chen et al., 2019b; Zhai et al., 2019).

3.2. Meteorologically driven changes in $PM_{2.5}$ concentrations from 2014 to 2018

$PM_{2.5}$ changes caused by meteorological variations are also presented in Fig. 2(a). Relative to 2014, $PM_{2.5}$ concentrations in 2018 were decreased by 8.7 μg m^{-3}, 2.6 μg m^{-3}, and 3.5 μg m^{-3} for NCP, YRD, and FWP owing to variations in meteorological conditions, contributing 27%, 13%, and 16%, respectively, of observed $PM_{2.5}$ decreases. Our estimated meteorological contribution in NCP (27%) to $PM_{2.5}$ decreases from 2014 to 2018 was higher than that obtained by Zhang et al. (2019a) (16%) and Zhang et al. (2019b) (13%), who focused on meteorological contribution to $PM_{2.5}$ decreases from 2013 to 2017. The discrepancy could be largely explained by favorable weather conditions in 2018. Relative to 2017, $PM_{2.5}$ concentrations over NCP in 2018 were decreased by 7.3 μg m^{-3} as a result of meteorological variations, accounting for 92% of $PM_{2.5}$ decreases from 2017 to 2018 (Fig. S4(a)).

Meteorologically driven $PM_{2.5}$ changes relative to previous year for each season are shown in Fig. S5 (a1)–(d1). Significant $PM_{2.5}$ decrease driven by meteorology for NCP in 2018 relative to 2017 was mainly contributed by the decreases in autumn and winter. Further investigation indicated that the increased PBLH in autumn and the decreased 2 m relative humidity (RH_2) in winter were the most influential meteorological variables, with relative contributions of 53% and 51% to meteorology-driven $PM_{2.5}$ decreases in autumn and winter, respectively.

The increased PBLH was conducive to enhance the atmosphere's ability to disperse particulate matters and improve $PM_{2.5}$ air quality (Miao et al., 2019). When water vapor was decreased, fewer secondary particles were formed through heterogeneous aqueous reactions especially during heavy pollution periods in winter, which eventually led to $PM_{2.5}$ decreases (Liu et al., 2018; Song et al., 2018).

3.3. Meteorologically driven trends of $PM_{2.5}$ concentrations over 2014–2018

Fig. 3 shows the annual and seasonal trends of $PM_{2.5}$ concentrations over 2014–2018. The observed five-year $PM_{2.5}$ trends in NCP, YRD, and FWP were −7.8 μg m^{-3} yr^{-1}, −4.7 μg m^{-3} yr^{-1}, and −4.7 μg m^{-3} yr^{-1}, with meteorological contributions of −2.0 μg m^{-3} yr^{-1} (26%), −0.5 μg m^{-3} yr^{-1} (10%), and −0.7 μg m^{-3} yr^{-1} (15%), respectively. Relative contributions of meteorological variations to observed $PM_{2.5}$ trends for four seasons were estimated to be −2%~41% in NCP, −2%~18% in YRD, and 2%~29% in FWP. The largest meteorology-driven trends of seasonal $PM_{2.5}$ concentrations for the three regions were −4.5 μg m^{-3} yr^{-1} in NCP during winter, −1.0 μg m^{-3} yr^{-1} in YRD during summer, and −1.6 μg m^{-3} yr^{-1} in FWP during winter, contributing 41%, 18%, and 29% of observed trends, respectively. The calculated meteorology-driven $PM_{2.5}$ trend for NCP during winter (−4.5 μg m^{-3} yr^{-1}) was consistent with that reported in Zhang et al. (2019a) and Zhai et al. (2019), which also focused on similar study periods and study areas.

We further identified the most influential meteorological factors to the three largest meteorology-driven $PM_{2.5}$ trends. For NCP in winter, the most influential meteorological factor, decreased RH_2 (−1.4% yr^{-1}), explained 55% of the $PM_{2.5}$ trend driven by meteorology. For YRD in summer, the increased 10 m wind speed (WS_{10}, +0.1 m s^{-1} yr^{-1}) was the dominant meteorological factor and contributed 33% of the meteorology-driven $PM_{2.5}$ trend. For FWP in winter, the increased daytime PBLH (PBLH_Daytime, +14.8 m yr^{-1}) contributed 50% of the meteorologically driven $PM_{2.5}$ trend. The decreased RH_2

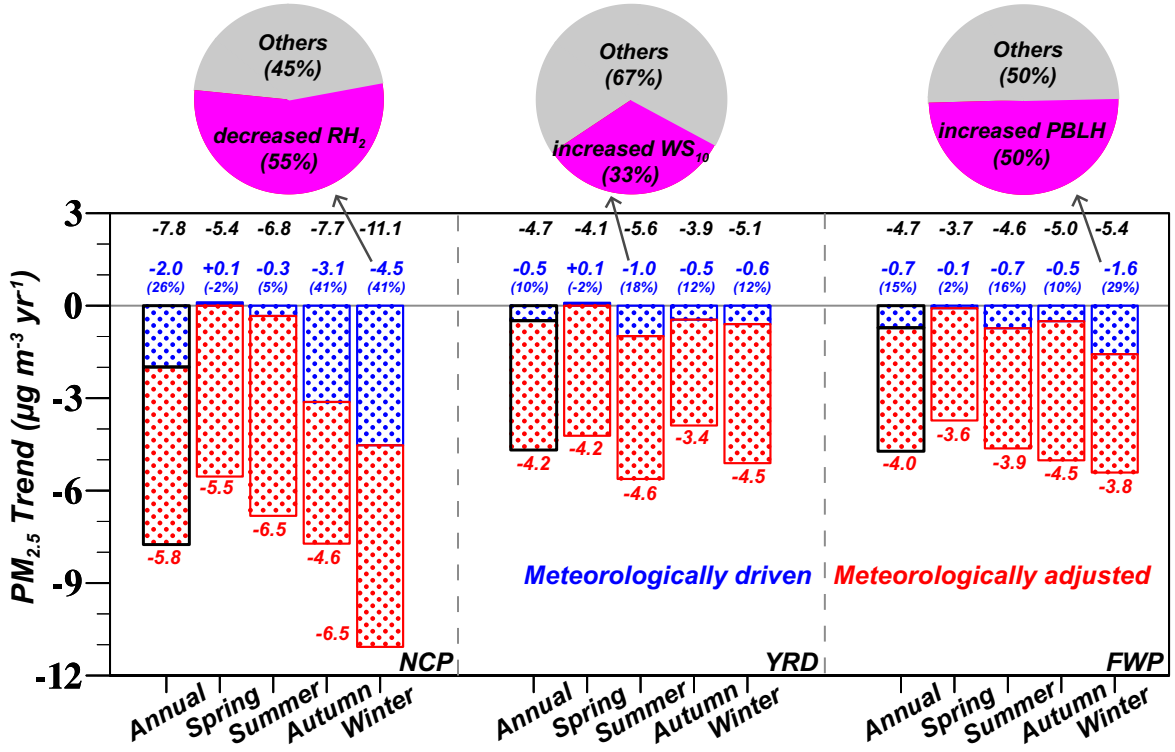

Fig. 3. Observed, meteorologically driven, and meteorologically adjusted trends of annual and seasonal $PM_{2.5}$ concentrations during 2014–2018 for NCP, YRD, and FWP. Black values represent observed trends; blue bars and values represent meteorologically driven trends; red bars and values represent non-meteorological (i.e., meteorologically adjusted) trends. The relative contributions of meteorological variations to observed trends are also shown in blue brackets. Pie charts exhibit the percentage contributions of the most influential meteorological factor (shown in purple) to meteorologically driven trends. The "PBLH" in the third pie chart refers to daytime PBLH. (For interpretation of the references to colour in this figure legend, the reader is referred to the web version of this article.)

and increased PBLH were beneficial meteorological conditions for the improvement of $PM_{2.5}$ air quality, as illustrated in Section 3.2. Southwesterly winds prevailed over eastern China in summer and the increased wind speeds were conducive to scavenging particulate matters in YRD (He et al., 2019).

4. Meteorological influences on O_3 air quality

4.1. Spatiotemporal characteristics of O_3 concentrations for 2014–2018

The spatial distribution of five-year (2014–2018) average MDA8 O_3 concentrations over China is presented in Fig. 1(b2). High values of MDA8 O_3 concentrations were also observed in NCP, YRD, and FWP, with the mean concentrations of 102.7 μg m^{-3}, 97.2 μg m^{-3}, and 92.8 μg m^{-3}, respectively. Fig. 1(b3) shows the spatial distribution of five-year trends in observed MDA8 O_3 concentrations over China. The observed MDA8 O_3 exhibited increasing trends across most of China but decreasing trends over part regions of southwestern and northeastern China. The average MDA8 O_3 trends for NCP, YRD, and FWP were +4.2 μg m^{-3} yr^{-1}, +3.9 μg m^{-3} yr^{-1}, and +6.6 μg m^{-3} yr^{-1}, respectively. Fig. 2(b) presents yearly MDA8 O_3 levels over 2014–2018 for the three regions. The MDA8 O_3 concentrations averaged over NCP, YRD, and FWP exhibited significant increases of 15.4 μg m^{-3} (16%), 12.5 μg m^{-3} (14%), and 25.9 μg m^{-3} (33%), respectively, from 2014 to 2018. Given that NMVOCs emissions changed little (Fig. S3), the decreased anthropogenic emissions of NO_x were regarded as a contributor to O_3 deterioration (Fu et al., 2019; Sun et al., 2019). A recent study conducted by Li et al. (2019) reported that the decreases in $PM_{2.5}$ since 2013 was also an important factor for O_3 increases by slowing down the aerosol sink of hydroperoxy radicals. In this study, the increases in MDA8 O_3 concentrations owing to non-meteorological variations (i.e., "meteorologically adjusted") from 2014 to 2018 in NCP, YRD, and FWP were 13.6 μg m^{-3}, 11.2 μg m^{-3}, and 22.1 μg m^{-3}, accounting for 88%, 90%, and 85%, respectively of observed O_3 increases (Fig. 2(b)). Similar contributions were reported in previous studies (Wang et al., 2019; Liu and Wang, 2020).

4.2. Meteorologically driven changes in O_3 concentrations from 2014 to 2018

As shown in Fig. 2(b), from 2014 to 2018, meteorology-driven changes in MDA8 O_3 concentrations were estimated to be +1.8 μg m^{-3}, +1.3 μg m^{-3}, and +3.8 μg m^{-3} for NCP, YRD, and FWP, contributing 12%, 10%, and 15%, respectively, of observed MDA8 O_3 increases. The large value of meteorology-driven increase (3.8 μg m^{-3}) from 2014 to 2018 in FWP was mainly attributed by the significant increase (2.8 μg m^{-3}) due to meteorological variation in 2018 relative to 2017 (Fig. S4(b)).

Fig. S5(a2)–(d2) present meteorologically driven MDA8 O_3 changes relative to previous year for each season. The significant MDA8 O_3 increase driven by meteorology for FWP from 2017 to 2018 was mainly contributed by the increases in spring and autumn. Further investigation indicated that the increased daily maximum 2 m temperature (T_2_Max) in spring and the increased PBLH_Daytime in autumn were the most influential meteorological variables, with relative contributions of 30% and 71% to meteorology-driven MDA8 O_3 increases in spring and autumn, respectively.

The increases in temperature enhanced the photochemical production of O_3 and accelerated biogenic emissions of O_3 precursors, which led to O_3 deterioration (Liu and Wang, 2020). With the development of PBL, more O_3 were transported downward from the upper atmosphere to the near surface, resulting in the increases in surface-layer O_3 concentrations (Sun et al., 2009; He et al., 2017).

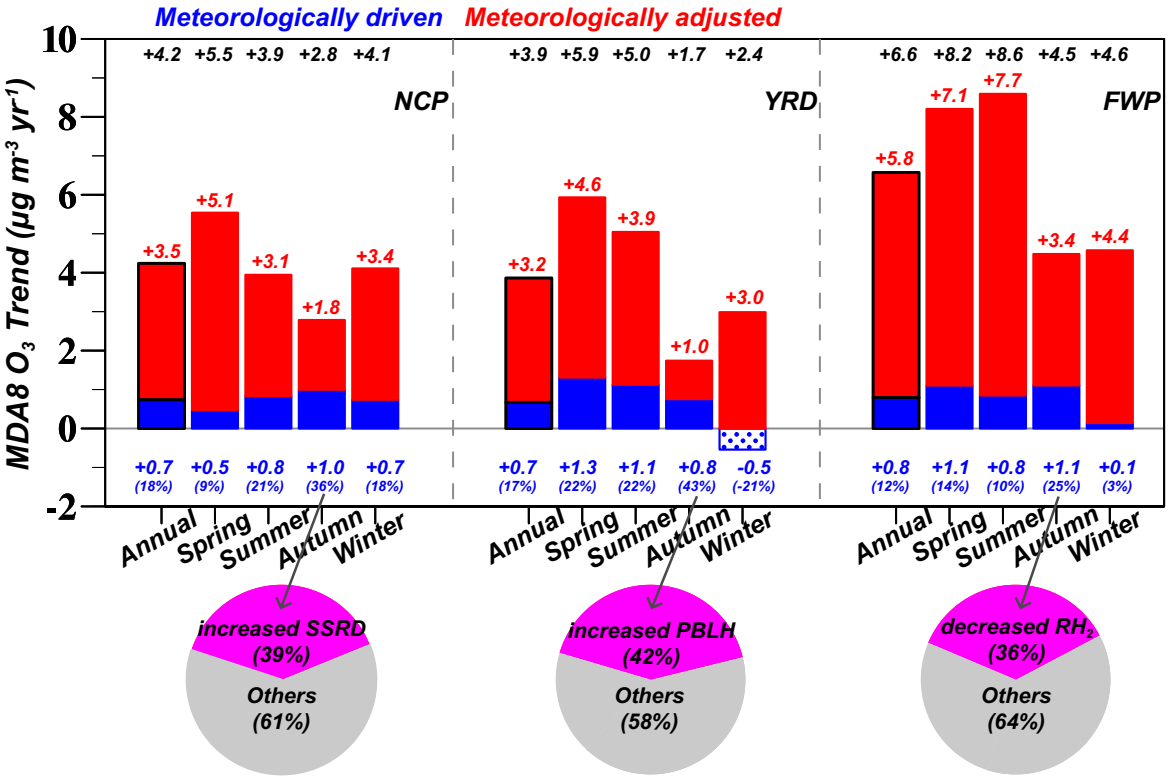

Fig. 4. Observed, meteorologically driven, and meteorologically adjusted trends of annual and seasonal MDA8 O_3 concentrations during 2014–2018 for NCP, YRD, and FWP. Black values represent observed trends; blue bars and values represent meteorologically driven trends; red bars and values represent non-meteorological (i.e., meteorologically adjusted) trends. The relative contributions of meteorological variations to observed trends are also shown in blue brackets. Pie charts exhibit the percentage contributions of the most influential meteorological factor (shown in purple) to meteorologically driven trends. The "SSRD" and "PBLH" in the first two pie charts refer to daytime SSRD and daytime PBLH. (For interpretation of the references to colour in this figure legend, the reader is referred to the web version of this article.)

4.3. Meteorologically driven trends of O_3 concentrations over 2014–2018

The annual and seasonal trends of MDA8 O_3 concentrations over 2014–2018 are shown in Fig. 4. The observed five-year MDA8 O_3 trends in NCP, YRD, and FWP were $+4.2$ μg m^{-3} yr^{-1}, $+3.9$ μg m^{-3} yr^{-1}, and $+6.6$ μg m^{-3} yr^{-1}, with meteorological contributions of $+0.7$ μg m^{-3} yr^{-1} (18%), $+0.7$ μg m^{-3} yr^{-1} (17%), and $+0.8$ μg m^{-3} yr^{-1} (12%), respectively. The percentage contributions of meteorological variations to observed MDA8 O_3 trends for four seasons were estimated to be 9% ~ 36% in NCP, −21%~43% in YRD, and 3%~25% in FWP. The largest contributions of meteorology to observed seasonal MDA8 O_3 trends for the three regions all occurred in autumn, with values of 36%, 43%, and 25% for NCP, YRD, and FWP.

Further investigation was conducted to identify the most influential meteorological factors to the three largest meteorology-driven MDA8 O_3 trends. For NCP in autumn, the increased daytime surface solar radiation downwards (SSRD_Daytime, $+28.9$ W m^{-2} yr^{-1}) was the dominant meteorological factor and contributed 39% of the meteorology-driven MDA8 O_3 trend. For YRD in autumn, the most influential meteorological factor, increased PBLH_Daytime ($+16.9$ m yr^{-1}), explained 42% of the MDA8 O_3 trend driven by meteorology. For FWP in autumn, the decreased RH_2 (-1.8% yr^{-1}) contributed 36% of the meteorology-driven MDA8 O_3 trend. Strong solar radiation promoted photochemical reactions and resulted in elevated O_3 levels (Chang et al., 2019). The development of PBL promoted the downward transportation of O_3 from upper atmosphere to near surface and caused the increases in surface-layer O_3 concentrations (Sun et al., 2009; He et al., 2017). Decreased relative humidity was always accompanied by lower cloud fraction which accelerated photochemical production of O_3 (Camalier et al., 2007). Some complicated chemistry processes inhibited O_3 formation under high humidity level, therefore decreased relative humidity led to O_3 increases (Yu, 2018).

5. Meteorological influences on $PM_{2.5}$– and O_3– related health burden

5.1. The $PM_{2.5}$–related mortality variations over 2014–2018

Annual variations in $PM_{2.5}$-related premature deaths during 2014–2018 relative to 2014 for NCP, YRD, and FWP are shown in Fig. 5 (a1)–(a3). The $PM_{2.5}$-related premature mortalities exhibited significant decreasing trends of −28.2 thousand yr^{-1}, −21.4 thousand yr^{-1}, and −20.3 thousand yr^{-1} for the three regions. The decreases in deaths were attributed to four contributing factors, i.e., meteorologically driven concentration variation (Met driven), meteorologically adjusted concentration variation (Met adjusted), population variation (Pop), and baseline mortality rate variation (BMR). The meteorology-driven decreases in $PM_{2.5}$ concentrations led to overall decreases in $PM_{2.5}$-related mortalities with trends of −7.4 thousand yr^{-1}, −2.2 thousand yr^{-1}, and −3.0 thousand yr^{-1} for NCP, YRD, and FWP, contributing 26%, 10%, and 15% of the total $PM_{2.5}$-related mortality trends. The meteorologically adjusted decreases in $PM_{2.5}$ concentrations, mainly attributed to reduced anthropogenic emissions, resulted in remarkable mortality decreases of −16.1~−20.1 thousand yr^{-1} across the three regions. Population growth exerted negative health effects and caused mortality increases of +2.3~+2.8 thousand yr^{-1}. The decreased BMR owing to improved medical conditions brought about positive health impacts and led to mortality decreases ranging from −3.3 thousand yr^{-1} to −3.6 thousand yr^{-1}.

We further examined the changes in $PM_{2.5}$-related deaths from 2014 to 2018, and the percentage contributions from the four driving factors in Table 2. The $PM_{2.5}$-related premature mortalities were estimated to be 479.8 thousand, 441.7 thousand, and 493.0 thousand in 2014 for NCP, YRD, and FWP, and decreased by 113.3 thousand, 90.5 thousand, and 89.6 thousand, respectively, from 2014 to 2018. The improved $PM_{2.5}$ air quality driven by meteorological variation led to overall health benefits, accounting for 29%, 13%, and 16% of the total avoided deaths for NCP, YRD, and FWP, respectively. Meteorologically adjusted decreases in $PM_{2.5}$ concentrations made considerable contributions to health benefits, with 72%~89% across the three regions. Population growth caused negative health effects and accounted for −12%~−10%. The decreased BMR contributed 9%~12% of the total avoided deaths. In summary, meteorologically driven decreases in $PM_{2.5}$ concentrations, meteorologically adjusted decreases in $PM_{2.5}$ concentrations, population growth, and reductions in baseline mortality rate, respectively, contributed 13%~29%, 72%~89%, −12%~−10%, and 9%~12%, to the total avoided $PM_{2.5}$-related mortalities between 2014 and 2018 for NCP, YRD, and FWP.

5.2. The O_3–related mortality variations over 2014–2018

Annual variations in O_3-related premature deaths during 2014–2018 relative to 2014 for NCP, YRD, and FWP are shown in Fig. 5 (b1)–(b3). The O_3-related premature mortalities exhibited significant increasing trends of +2.1 thousand yr^{-1}, +2.9 thousand yr^{-1}, and +4.8 thousand yr^{-1} for the three regions. The meteorology-driven increases in MDA8 O_3 concentrations led to overall increases in O_3-related mortalities with trends of +0.5 thousand yr^{-1}, +0.9 thousand yr^{-1}, and +0.7 thousand yr^{-1} for NCP, YRD, and FWP, contributing 24%, 31%, and 15% of the total O_3-related mortality trends. The meteorologically adjusted increases in MDA8 O_3 concentrations resulted in remarkable mortality increases of +1.9~+4.5 thousand yr^{-1} across the three regions. Population growth exerted negative health effects and caused mortality increases of +0.2~+0.3 thousand yr^{-1}. The decreased BMR owing to health medical conditions brought about positive health impacts and led to mortality decreases ranging from −0.4 thousand yr^{-1} to −0.6 thousand yr^{-1}.

We further examined the changes in O_3-related deaths from 2014 to 2018, and the percentage contributions from the four driving factors in Table 2. The O_3-related excess deaths were evaluated to be 49.2 thousand, 38.5 thousand, and 34.6 thousand in 2014 for NCP, YRD, and FWP, and increased by 6.5 thousand, 9.2 thousand, and 18.0 thousand, respectively, from 2014 to 2018. The deteriorated O_3 air quality induced by meteorological variation caused overall health burden, accounting for 17%, 29%, and 16% of the total increased deaths for NCP, YRD, and FWP, respectively. The meteorologically adjusted increases in MDA8 O_3 concentrations made great contributions to the health burden, with 79%~98% across the three regions. Population growth also led to increased deaths and accounted for 3%~17%. The decreased BMR contributed −32%~−8% of the total increased deaths. Overall, meteorologically driven increases in MDA8 O_3 levels, meteorologically adjusted increases in MDA8 O_3 levels, population growth, and reductions in baseline mortality rate, respectively, contributed 16%~29%, 79%~98%, 3%~17%, and −32%~−8%, to the total increased O_3-related mortalities from 2014 to 2018 for NCP, YRD, and FWP.

6. Conclusions

We developed multiple linear regression (MLR) models to identify meteorological influences on the trends in $PM_{2.5}$ and O_3 concentrations and associated health burden for three regions (NCP, YRD, and FWP) in China over 2014–2018. The contributions of the most influential meteorological factors to $PM_{2.5}$ and O_3 trends were highlighted.

The observed five-year $PM_{2.5}$ trends in NCP, YRD, and FWP were estimated to be -7.8 μg m^{-3} yr^{-1}, -4.7 μg m^{-3} yr^{-1}, and -4.7 μg m^{-3} yr^{-1}, with meteorological contributions of -2.0 μg m^{-3} yr^{-1} (26%), -0.5 μg m^{-3} yr^{-1} (10%), and -0.7 μg m^{-3} yr^{-1} (15%), respectively. The largest meteorological contributions to seasonal $PM_{2.5}$ trends for the three regions were 41% in NCP during winter, 18% in YRD during summer, and 29% in FWP during winter. The decreased RH_2, the increased WS_{10}, and increased daytime PBLH were the most influential

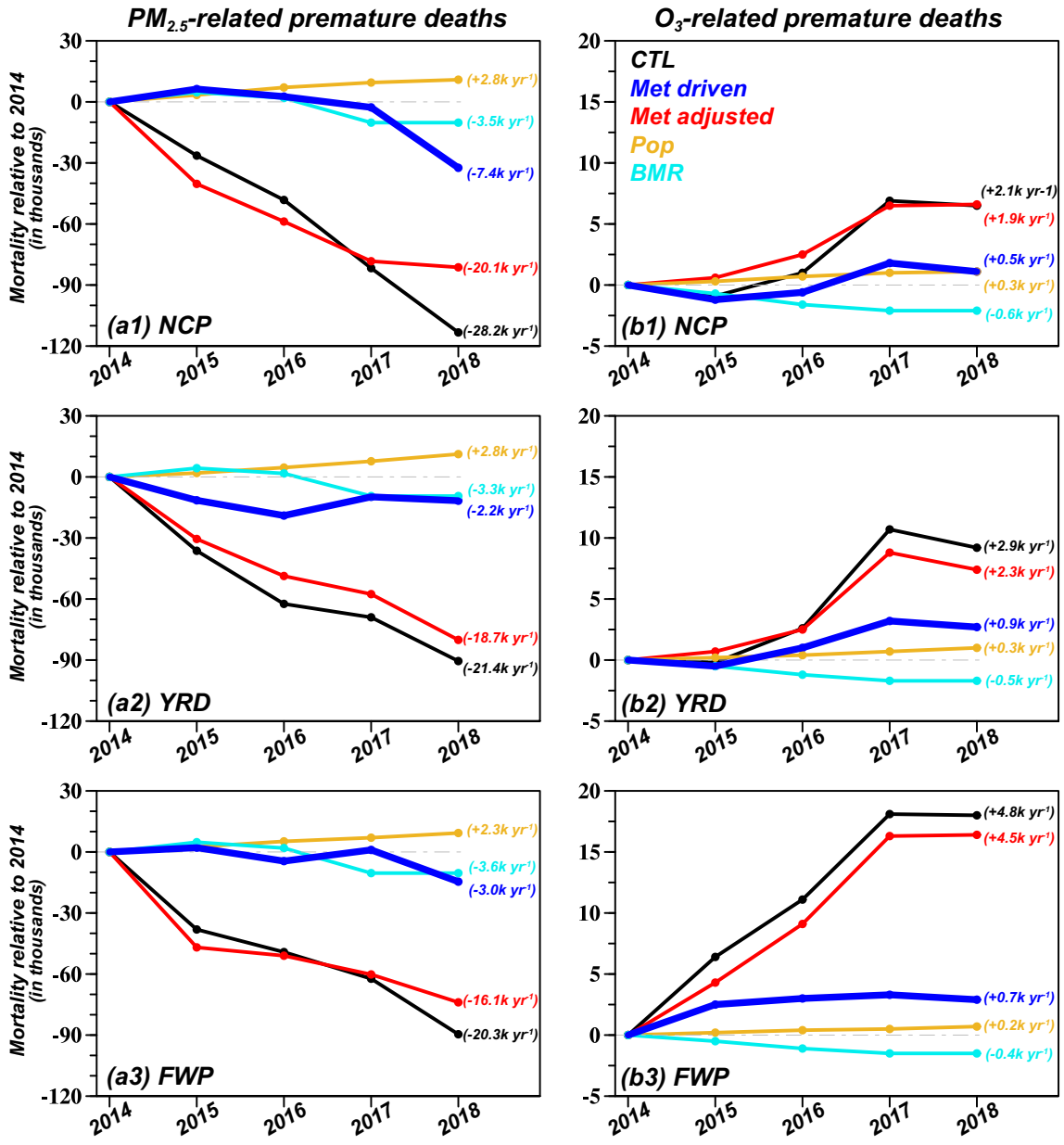

Fig. 5. Annual variations in (a1–a3) $PM_{2.5}$- and (b1–b3) O_3-related premature deaths during 2014–2018 relative to 2014 for NCP, YRD, and FWP, under normal condition (CTL, shown in black line), owing to meteorologically driven concentration variation alone (Met driven, shown in dark blue line), owing to meteorologically adjusted concentration variation alone (Met adjusted, shown in red line), owing to population variation alone (Pop, shown in brown line), owing to baseline mortality rate variation alone (BMR, shown in light blue line). The 5-year trends calculated under each condition are presented in values with corresponding colors. The BMR data in 2018 are the same as those in 2017 because of the unavailability of the BMR data in 2018 during the conduct of this study. (For interpretation of the references to colour in this figure legend, the reader is referred to the web version of this article.)

Table 2
Estimated $PM_{2.5}$- and O_3-related premature deaths in 2014 (in thousands, 95% confidence intervals), the changed deaths from 2014 to 2018 (in thousands, 95% confidence intervals), and the percentage contributions to the changed deaths from four factors, i.e., meteorologically driven concentration (Conc) change (Met driven), meteorologically adjusted Conc change (Met adjusted), population (Pop) change, and baseline mortality rate (BMR) change.

Region		Deaths (in 2014)	Changed deaths (2018–2014)	Conc change alone		Pop change alone (%)	BMR change alone (%)
				Met driven (%)	Met adjusted (%)		
$PM_{2.5}$	NCP	479.8 (465.7, 493.8)	−113.3 (−116.1, −110.6)	29	72	−10	9
	YRD	441.7 (428.4, 455.1)	−90.5 (−92.8, −88.2)	13	89	−12	10
	FWP	493.0 (478.4, 507.6)	−89.6 (−91.8, −87.4)	16	82	−10	12
O_3	NCP	49.2 (47.8, 50.6)	+6.5 (+6.3, +6.6)	17	98	17	−32
	YRD	38.5 (37.4, 39.7)	+9.2 (+8.9, +9.4)	29	79	10	−18
	FWP	34.6 (33.6, 35.7)	+18.0 (+17.6, +18.4)	16	89	3	−8

meteorological factors, and contributed 55%, 33%, and 50%, respectively, of the three largest meteorology-driven seasonal $PM_{2.5}$ trends.

The observed five-year MDA8 O_3 trends in NCP, YRD, and FWP were calculated to be $+4.2\ \mu g\ m^{-3}\ yr^{-1}$, $+3.9\ \mu g\ m^{-3}\ yr^{-1}$, and $+6.6\ \mu g\ m^{-3}\ yr^{-1}$, with meteorological contributions of $+0.7\ \mu g\ m^{-3}\ yr^{-1}$ (18%), $+0.7\ \mu g\ m^{-3}\ yr^{-1}$ (17%), and $+0.8\ \mu g\ m^{-3}\ yr^{-1}$ (12%), respectively. The largest meteorological contributions to seasonal MDA8 O_3 trends for the three regions all occurred in autumn, with values of 36%, 43%, and 25% for NCP, YRD, and FWP. The increased daytime SSRD, the increased daytime PBLH, and the decreased RH_2 were the most influential meteorological factors, and contributed 39%, 42%, and 36%, respectively, of the three largest meteorology-driven seasonal MDA8 O_3 trends.

The $PM_{2.5}$-related premature mortalities exhibited significant decreasing trends of -28.2 thousand yr^{-1}, -21.4 thousand yr^{-1}, and -20.3 thousand yr^{-1} for NCP, YRD, and FWP during 2014–2018. The meteorology-driven decreases in $PM_{2.5}$ concentrations led to overall decreases in $PM_{2.5}$-related mortalities with trends of -7.4 thousand yr^{-1}, -2.2 thousand yr^{-1}, and -3.0 thousand yr^{-1} for the three regions. The O_3-related premature mortalities exhibited significant increasing trends of $+2.1$ thousand yr^{-1}, $+2.9$ thousand yr^{-1}, and $+4.8$ thousand yr^{-1} for NCP, YRD, and FWP over 2014–2018. The meteorology-driven increases in MDA8 O_3 concentrations led to overall increases in O_3-related mortalities with trends of $+0.5$ thousand yr^{-1}, $+0.9$ thousand yr^{-1}, and $+0.7$ thousand yr^{-1} for the three regions.

The findings from the present study emphasize the important role of meteorology in $PM_{2.5}$ and O_3 air quality and associated health burden over China, and have important implications for China's air quality planning. In particular, the adverse effects of meteorology on O_3 air quality and O_3-related health burden should be considered when making ozone pollution control strategy. More efforts in emission control should be taken to offset the adverse effects on ozone caused by meteorology.

Meteorological impacts on air quality vary by regions in China, and the meteorology-driven changes can be comparable or even more significant than those caused by anthropogenic emissions (Liu and Wang, 2020). Therefore, it is of great importance to identify the most influential meteorological variables for $PM_{2.5}$ (O_3) changes over the whole China since clean air actions. The trends of the dominant meteorological variables may be used as a reference metric for China's air quality planning. Air pollution can be affected by meteorological variations on multiple timescales (e.g., long-term trend and day-to-day variability) (Tai et al., 2010; Seo et al., 2018). In this study, meteorological influences on five-year trends have been quantified by MLR models. Understanding the synoptic-scale correlations between $PM_{2.5}$ (O_3) levels and meteorological variables are also important to air quality (Henneman et al., 2015; Han et al., 2020). The Kolmogorov-Zurbenko (KZ) filter can be used to decompose the time series into different timescales and quantify the effects of short-term meteorological fluctuations on air pollution, which will be further issues that need to be addressed.

Data availability

All data used in this study can be accessed publicly. Meteorological variables were obtained from the European Centre (https://apps.ecmwf.int/datasets/). Network observations of $PM_{2.5}$ and O_3 concentrations were collected from the China National Environmental Monitoring Center (http://106.37.208.233:20035/). Baseline mortality rates of diseases were taken from the Global Burden of Disease study (GBD) results tool (http://ghdx.healthdata.org/gbd-results-tool). The provincial population data were downloaded from the China Statistical Yearbook (http://www.stats.gov.cn/tjsj/ndsj/). The gridded population data were from Global Population for World (GPW) dataset (https://sedac.ciesin.columbia.edu/data/collection/gpw-v4/sets/browse).

CRediT authorship contribution statement

Lei Chen: Conceptualization, Methodology, Software, Data curation, Visualization, Writing - original draft. **Jia Zhu:** Investigation, Formal analysis, Writing - review & editing. **Hong Liao:** Writing - review & editing, Supervision, Funding acquisition. **Yang Yang:** Resources, Validation, Supervision. **Xu Yue:** Formal analysis, Supervision.

Declaration of competing interest

The authors declare that they have no known competing financial interests or personal relationships that could have appeared to influence the work reported in this paper.

Acknowledgements

This work was supported by the National Key R&D Program of China [grant number 2019YFA0606804]; the National Natural Science Foundation of China [grant number 91744311]; the University Natural Science Research Foundation of Jiangsu Province [grant number 18KJB170012]; the China Postdoctoral Science Foundation [grant number 2019M650117]; and the Startup Foundation for Introducing Talent of NUIST [grant number 2018r007]. We appreciate the reviewers for their constructive comments and thoughtful suggestions.

Appendix A. Supplementary data

Supplementary data to this article can be found online at https://doi.org/10.1016/j.scitotenv.2020.140837.

References

Akaike, H., 1969. Fitting autoregressive models for prediction. Ann. Inst. Stat. Math. 21 (2), 243–247. https://doi.org/10.1007/BF02532251.

Altland, H.W., 1999. Regression analysis: statistical modeling of a response variable. Technometrics 41 (4), 367–368. https://doi.org/10.1080/00401706.1999.10485936.

Anenberg, S.C., Horowitz, L.W., Tong, D.Q., West, J.J., 2010. An estimate of the global burden of anthropogenic ozone and fine particulate matter on premature human mortality using atmospheric modeling. Environ. Health Perspect. 118, 1189–1195. https://doi.org/10.1289/ehp.0901220.

Boogaard, H., Walker, K., Cohen, A.J., 2019. Air pollution: the emergence of a major global health risk factor. Int. Health 11, 417–421. https://doi.org/10.1093/inthealth/ihz078.

Burnett, R., Chen, H., Szyszkowicz, M., Fann, N., Hubbell, B., Pope, C.A., Spte, J.S., Brauer, M., Cohen, A., Weichenthal, S., Coggins, J., Di, Q., Brunekreef, B., Frostad, F., Lim, S.S., Kan, H., Walker, K.d., Thurston, G.D., Hayes, R.b., Lim, C.C., Turner, M.C., Jerrett, M., Krewski, D., Gapstur, S.M., Diver, W.R., Ostro, B., Goldberg, D., Crouse, D.L., Martin, R.V., Peters, P., Pinault, L., Tjepkema, M., Donkelaar, A., Villeneuve, P.J., Miller, A.B., Yin, P., Zhou, M., Wang, L., Janssen, N.A.H., Marra, M., Atkinson, R.W., Tsang, H., Thach, T.Q., Cannon, J.B., Allen, R.T., Hart, J.E., Laden, F., Cesaroni, G., Forastisere, F., Weinmayr, G., Jaensch, A., Nagel, G., Concin, H., Spadaro, J.V., 2018. Global estimates of mortality associated with longterm exposure to outdoor fine particulate matter. Proc. Natl. Acad. Sci. U.S.A. 115 (38), 9592–9597. https://doi.org/10.1073/pnas.1803222115.

Camalier, L., Cox, W., Dolwick, P., 2007. The effects of meteorology on ozone in urban areas and their use in assessing ozone trends. Atmos. Environ. 41, 7127–7137. https://doi.org/10.1016/j.atmosenv.2007.04.061.

Chang, L., Xu, J., Tie, X., Gao, W., 2019. The impact of climate change on the Western Pacific subtropical high and the related ozone pollution in Shanghai, China. Sci. Rep. 9. https://doi.org/10.1038/s41598-019-53103-7.

Che, H., Gui, K., Xia, X., Wang, Y., Holben, B.N., Goloub, P., Cuevas-Agulló, E., Wang, H., Zheng, Y., Zhao, H., Zhang, X., 2019. Large contribution of meteorological factors to inter-decadal changes in regional aerosol optical depth. Atmos. Chem. Phys. 19, 10497–10523. https://doi.org/10.5194/acp-19-10497-2019.

Chen, Z., Chen, D., Kwan, M.-P., Chen, B., Gao, B., Zhuang, Y., Li, R., Xu, B., 2019a. The control of anthropogenic emissions contributed to 80% of the decrease in $PM_{2.5}$ concentrations in Beijing from 2013 to 2017. Atmos. Chem. Phys. 19, 13519–13533. https://doi.org/10.5194/acp-19-13519-2019.

Chen, L., Zhu, J., Liao, H., Gao, Y., Qiu, Y., Zhang, M., Liu, Z., Li, N., Wang, Y., 2019b. Assessing the formation and evolution mechanisms of severe haze pollution in the Beijing–Tianjin–Hebei region using process analysis. Atmos. Chem. Phys. 19, 10845–10864. https://doi.org/10.5194/acp-19-10845-2019.

Chen, X., Zhong, B., Huang, F., Wang, X., Sarkar, S., Jia, S., Deng, X., Chen, D., Shao, M., 2020. The role of natural factors in constraining long-term tropospheric ozone trends over Southern China. Atmos. Environ. 220, 117060. https://doi.org/10.1016/j.atmosenv.2019.117060.

Dang, R., Liao, H., 2019. Radiative forcing and health impact of aerosols and ozone in China as the consequence of clean air actions over 2012–2017. Geophys. Res. Lett. 46 (12), 511–512. https://doi.org/10.1029/2019GL084605.
Ding, D., Xing, J., Wang, S., Chang, X., Hao, J., 2019a. Impacts of emissions and meteorological changes on China's ozone pollution in the warm seasons of 2013 and 2017. Front. Environ. Sci. Eng. 13. https://doi.org/10.1007/s11783-019-1160-1.
Ding, D., Xing, J., Wang, S., Liu, K., Hao, J., 2019b. Estimated contributions of emissions controls, meteorological factors, population growth, and changes in baseline mortality to reductions in ambient $PM_{2.5}$ and O_3-related mortality in China, 2013-2017. Environ. Health Perspect. 127, 67009. https://doi.org/10.1289/EHP4157.
Fan, H., Zhao, C., Yang, Y., 2020. A comprehensive analysis of the spatio-temporal variation of urban air pollution in China during 2014-2018. Atmos. Environ. 220, 117066. https://doi.org/10.1016/j.atmosenv.2019.117066.
Fu, Y., Liao, H., Yang, Y., 2019. Interannual and decadal changes in tropospheric ozone in China and the associated chemistry–climate interactions: a review. Adv. Atmos. Sci. 36 (9), 975–993. https://doi.org/10.1007/s00376-019-8216-9.
Gao, Y., Zhang, M., Liu, Z., Wang, L., Wang, P., Xia, X., Tao, M., Zhu, L., 2015. Modeling the feedback between aerosol and meteorological variables in the atmospheric boundary layer during a severe fog–haze event over the North China Plain. Atmos. Chem. Phys. 15, 4279–4295. https://doi.org/10.5194/acp-15-4279-2015.
Gao, M., Carmichael, G.R., Saide, P.E., Lu, Z., Yu, M., Streets, D.G., Wang, Z., 2016. Response of winter fine particulate matter concentrations to emission and meteorology changes in North China. Atmos. Chem. Phys. 16, 11837–11851. https://doi.org/10.5194/acp-16-11837-2016.
Gao, M., Liu, Z., Zheng, B., Ji, D., Sherman, P., Song, S., Xin, J., Liu, C., Wang, Y., Zhang, Q., Xing, J., Jiang, J., Wang, Z., Carmichael, G.R., McElroy, M.B., 2020. China's emission control strategies have suppressed unfavorable influences of climate on wintertime $PM_{2.5}$ concentrations in Beijing since 2002. Atmos. Chem. Phys. 20, 1497–1505. https://doi.org/10.5194/acp-20-1497-2020.
Han, X., Zhang, M., Gao, J., Wang, S., Chai, F., 2014. Modeling analysis of the seasonal characteristics of haze formation in Beijing. Atmos. Chem. Phys. 14, 10231–10248. https://doi.org/10.5194/acp-14-10231-2014.
Han, H., Liu, J., Shu, L., Wang, T., Yuan, H., 2020. Local and synoptic meteorological influences on daily variability in summertime surface ozone in eastern China. Atmos. Chem. Phys. 20, 203–222. https://doi.org/10.5194/acp-20-203-2020.
He, J., Gong, S., Yu, Y., Yu, L., Wu, L., Mao, H., Song, C., Zhao, S., Liu, H., Li, X., Li, R., 2017. Air pollution characteristics and their relation to meteorological conditions during 2014-2015 in major Chinese cities. Environ. Pollut. 223, 484–496. https://doi.org/10.1016/j.envpol.2017.01.050.
He, L., Lin, A., Chen, X., Zhou, H., Zhou, Z., He, P., 2019. Assessment of MERRA-2 surface $PM_{2.5}$ over the Yangtze River basin: ground-based verification, spatiotemporal distribution and meteorological dependence. Remote Sens. 11, 460. https://doi.org/10.3390/rs11040460.
Henneman, L.R.F., Holmes, H.A., Mulholland, J.A., Russel, A.G., 2015. Meteorological detrending of primary and secondary pollutant concentrations: method application and evaluation using long-term (2000−2012) data in Atlanta. Atmos. Environ. 119, 201–210. https://doi.org/10.1016/j.atmosenv.2015.08.007.
Huang, J., Pan, X., Guo, X., Li, G., 2018a. Health impact of China's air pollution prevention and control action plan: an analysis of national air quality monitoring and mortality data. Lancet Planet. Health 2, 313–323. https://doi.org/10.1016/s2542-5196(18)30141-4.
Huang, X., Wang, Z., Ding, A., 2018b. Impact of aerosol-PBL interaction on haze pollution: multiyear observational evidences in North China. GeoRL 45, 8596–8603. https://doi.org/10.1029/2018gl079239.
Jacob, D.J., Winner, D.A., 2009. Effect of climate change on air quality. Atmos. Environ. 43, 51–63. https://doi.org/10.1016/j.atmosenv.2008.09.051.
Jerrett, M., Burnett, R.T., Pope, C.A., Ito, K., Thurston, G., Krewski, D., Shi, Y., Calle, E., Thun, M., 2009. Long-term ozone exposure and mortality. N. Engl. J. Med. 360 (11), 1085–1095. https://doi.org/10.1056/NEJMoa0803894.
Kutner, M., Nachtsheim, C., Neter, J., 2004. Applied Linear Regression Models. Richard D. Irwin, Inc, Homewood, Illinois.
Lee, Y.C., Shindell, D.T., Faluvegi, G., Wenig, M., Lam, Y.F., Ning, Z., Hao, S., Lai, C.S., 2014. Increase of ozone concentrations, its temperature sensitivity and the precursor factor in South China. Tellus Ser. B Chem. Phys. Meteorol. 66, 23455. https://doi.org/10.3402/tellusb.v66.23455.
Lelieveld, J., Evans, J.S., Fnais, M., Giannadaki, D., Pozzer, A., 2015. The contribution of outdoor air pollution sources to premature mortality on a global scale. Nature 525, 367–371. https://doi.org/10.1038/nature15371.
Leung, D.M., Tai, A.P.K., Mickley, L.J., Moch, J.M., van Donkelaar, A., Shen, L., Martin, R.V., 2018. Synoptic meteorological modes of variability for fine particulate matter ($PM_{2.5}$) air quality in major metropolitan regions of China. Atmos. Chem. Phys. 18, 6733–6748. https://doi.org/10.5194/acp-18-6733-2018.
Li, K., Jacob, D.J., Liao, H., Shen, L., Zhang, Q., Bates, K.H., 2019. Anthropogenic drivers of 2013–2017 trends in summer surface ozone in China. Proc. Natl. Acad. Sci. U.S.A. 116, 422–427. https://doi.org/10.1073/pnas.1812168116.
Liu, Y., Wang, T., 2020. Worsening urban ozone pollution in China from 2013 to 2017-part 1: the complex and varying roles of meteorology. Atmos. Chem. Phys. Discuss. https://doi.org/10.5194/acp-2019-1120.
Liu, Q., Jia, X., Quan, J., Li, J., Li, X., Wu, Y., Chen, D., Wang, Z., Liu, Y., 2018. New positive feedback mechanism between boundary layer meteorology and secondary aerosol formation during severe haze events. Sci. Rep. 8, 6095. https://doi.org/10.1038/s41598-018-24366-3.
Lou, S., Liao, H., Yang, Y., Mu, Q., 2015. Simulation of the interannual variations of tropospheric ozone over China: roles of variations in meteorological parameters and anthropogenic emissions. Atmos. Environ. 122, 839–851. https://doi.org/10.1016/j.atmosenv.2015.08.081.
Ma, Z., Xu, J., Quan, W., Zhang, Z., Lin, W., Xu, X., 2016. Significant increase of surface ozone at a rural site, north of eastern China. Atmos. Chem. Phys. 16, 3969–3977. https://doi.org/10.5194/acp-16-3969-2016.
Malley, C.S., Henze, D.K., Kuylenstierna, J.C.I., Vallack, H.W., Davila, Y., Anenberg, S.C., Turner, M.C., Ashmore, M.R., 2017. Updated global estimates of respiratory mortality in adults ≥ 30 years of age attributable to long-term ozone exposure. Environ. Health Perspect. 125, 087021. https://doi.org/10.1289/EHP1390.
Miao, Y., Li, J., Miao, S., Che, H., Wang, Y., Zhang, X., Zhu, R., Liu, S., 2019. Interaction between planetary boundary layer and $PM_{2.5}$ pollution in megacities in China: a review. Current Pollution Reports 5, 261–271. https://doi.org/10.1007/s40726-019-00124-5.
Nieuwenhuijsen, M.J., Gascon, M., Martinez, D., Ponjoan, A., Blanch, J., Garcia-Gil, M.D.M., Ramos, R., Foraster, M., Mueller, N., Espinosa, A., Cirach, M., Khreis, H., Dadvand, P., Basagana, X., 2018. Air pollution, noise, blue space, and green space and premature mortality in Barcelona: a mega cohort. Int. J. Environ. Res. Public Health 15. https://doi.org/10.3390/ijerph15112405.
Querol, X., Alastuey, A., Pandolfi, M., Reche, C., Perez, N., Minguillon, M.C., Moreno, T., Viana, M., Escudero, M., Orio, A., Pallares, M., Reina, F., 2014. 2001-2012 trends on air quality in Spain. Sci. Total Environ. 490, 957–969. https://doi.org/10.1016/j.scitotenv.2014.05.074.
Racherla, P.N., Adams, P.J., 2006. Sensitivity of global tropospheric ozone and fine particulate matter concentrations to climate change. J. Geophys. Res.-Atmos. 111. https://doi.org/10.1029/2005jd006939.
Seo, J., Park, D.-S.R., Kim, J.Y., Youn, D., Lim, Y.B., Kim, Y., 2018. Effects of meteorology and emissions on urban air quality: a quantitative statistical approach to long-term records (1999–2016) in Seoul, South Korea. Atmos. Chem. Phys. 18, 16121–16137. https://doi.org/10.5194/acp-18-16121-2018.
Shen, L., Mickley, L.J., Murray, L.T., 2017. Influence of 2000–2050 climate change on particulate matter in the United States: results from a new statistical model. Atmos. Chem. Phys. 17, 4355–4367. https://doi.org/10.5194/acp-17-4355-2017.
Silva, R.A., Adelman, Z., Fry, M.M., West, J.J., 2016. The impact of individual anthropogenic emissions sectors on the global burden of human mortality due to ambient air pollution. Environ. Health Perspect. 124, 1776–1784. https://doi.org/10.1289/EHP177.
Silva, R.A., West, J.J., Lamarque, J.F., Shindell, D.T., Collins, W.J., Faluvegi, G., Folberth, G.A., Horowitz, L.W., Nagashima, T., Naik, V., Rumbold, S.T., Sudo, K., Takemura, T., Bergmann, D., Cameron-Smith, P., Doherty, R.M., Josse, B., MacKenzie, I.A., Stevenson, D.S., Zeng, G., 2017. Future global mortality from changes in air pollution attributable to climate change. Nat. Clim. Chang. 7, 647–651. https://doi.org/10.1038/nclimate3354.
Song, S., Gao, M., Xu, W., Shao, J., Shi, G., Wang, S., Wang, Y., Sun, Y., McElroy, M.B., 2018. Fine-particle pH for Beijing winter haze as inferred from different thermodynamic equilibrium models. Atmos. Chem. Phys. 18, 7423–7438. https://doi.org/10.5194/acp-18-7423-2018.
Sun, Y., Wang, Y., Zhang, C., 2009. Vertical observations and analysis of $PM_{2.5}$, O_3, and NO_x at Beijing and Tianjin from towers during summer and Autumn 2006. Adv. Atmos. Sci. 27, 123–136. https://doi.org/10.1007/s00376-009-8154-z.
Sun, L., Xue, L., Wang, Y., Li, L., Lin, J., Ni, R., Yan, Y., Chen, L., Li, J., Zhang, Q., Wang, W., 2019. Impacts of meteorology and emissions on summertime surface ozone increases over central eastern China between 2003 and 2015. Atmos. Chem. Phys. 19, 1455–1469. https://doi.org/10.5194/acp-19-1455-2019.
Tai, A.P.K., Mickley, L.J., Jacob, D.J., 2010. Correlations between fine particulate matter ($PM_{2.5}$) and meteorological variables in the United States: implications for the sensitivity of $PM_{2.5}$ to climate change. Atmos. Environ. 44, 3976–3984. https://doi.org/10.1016/j.atmosenv.2010.06.060.
Tai, A.P.K., Mickley, L.J., Jacob, D.J., 2012. Impact of 2000-2050 climate change on fine particulate matter ($PM_{2.5}$) air quality inferred from a multi-model analysis of meteorological modes. Atmos. Chem. Phys. 12, 11329–11337. https://doi.org/10.5194/acp-12-11329-2012.
Tao, M., Wang, L., Chen, L., Wang, Z., Tao, J., 2020. Reversal of aerosol properties in eastern China with rapid decline of anthropogenic emissions. Remote Sens. 12, 523. https://doi.org/10.3390/rs12030523.
Turner, M.C., Jerrett, M., Pope 3rd, C.A., Krewski, D., Gapstur, S.M., Diver, W.R., Beckerman, B.S., Marshall, J.D., Su, J., Crouse, D.L., Burnett, R.T., 2016. Long-term ozone exposure and mortality in a large prospective study. Am. J. Respir. Crit. Care Med. 193, 1134–1142. https://doi.org/10.1164/rccm.201508-1633OC.
Unger, N., Shindell, D.T., Koch, D.M., Amann, M., Cofala, J., Streets, D.G., 2006. Influences of man-made emissions and climate changes on tropospheric ozone, methane, and sulfate at 2030 from a broad range of possible futures. J. Geophys. Res.-Atmos. 111. https://doi.org/10.1029/2005jd006518.
Wang, X., Dickinson, R.E., Su, L., Zhou, C., Wang, K., 2018. $PM_{2.5}$ pollution in China and how it has been exacerbated by terrain and meteorological conditions. Bull. Am. Meteorol. Soc. 99, 105–119. https://doi.org/10.1175/bams-d-16-0301.1.
Wang, P., Guo, H., Hu, J., Kota, S.H., Ying, Q., Zhang, H., 2019. Responses of $PM_{2.5}$ and O_3 concentrations to changes of meteorology and emissions in China. Sci. Total Environ. 662, 297–306. https://doi.org/10.1016/j.scitotenv.2019.01.227.
Xie, Y., Dai, H., Zhang, Y., Wu, Y., Hanaoka, T., Masui, T., 2019. Comparison of health and economic impacts of $PM_{2.5}$ and ozone pollution in China. Environ. Int. 130, 104881. https://doi.org/10.1016/j.envint.2019.05.075.
Yang, Y., Russell, L.M., Lou, S., Liao, H., Guo, J., Liu, Y., Singh, B., Ghan, S.J., 2017. Dust-wind interactions can intensify aerosol pollution over eastern China. Nat. Commun. 8, 15333. https://doi.org/10.1038/ncomms15333.
Yang, L., Luo, H., Yuan, Z., Zheng, J., Huang, Z., Li, C., Lin, X., Louie, P.K.K., Chen, D., Bian, Y., 2019. Quantitative impacts of meteorology and precursor emission changes on the long-term trend of ambient ozone over the Pearl River Delta, China, and implications for ozone control strategy. Atmos. Chem. Phys. 19, 12901–12916. https://doi.org/10.5194/acp-19-12901-2019.

Yu, S., 2018. Fog geoengineering to abate local ozone pollution at ground level by enhancing air moisture. Environ. Chem. Lett. 17, 565–580. https://doi.org/10.1007/s10311-018-0809-5.

Yue, X., Unger, N., Harper, K., Xia, X., Liao, H., Zhu, T., Xiao, J., Feng, Z., Li, J., 2017. Ozone and haze pollution weakens net primary productivity in China. Atmos. Chem. Phys. 17, 6073–6089. https://doi.org/10.5194/acp-17-6073-2017.

Zhai, S., Jacob, D.J., Wang, X., Shen, L., Li, K., Zhang, Y., Gui, K., Zhao, T., Liao, H., 2019. Fine particulate matter ($PM_{2.5}$) trends in China, 2013-2018: separating contributions from anthropogenic emissions and meteorology. Atmos. Chem. Phys. 19, 11031–11041. https://doi.org/10.5194/acp-19-11031-2019.

Zhang, Z., Wang, K., 2020. Stilling and recovery of the surface wind speed based on observation, reanalysis, and geostrophic wind theory over China from 1960 to 2017. J. Clim. 33, 3989–4008. https://doi.org/10.1175/jcli-d-19-0281.1.

Zhang, L., Liao, H., Li, J., 2010. Impacts of Asian summer monsoon on seasonal and interannual variations of aerosols over eastern China. J. Geophys. Res.-Atmos. 115. https://doi.org/10.1029/2009jd012299.

Zhang, Y., West, J.J., Mathur, R., Xing, J., Hogrefe, C., Roselle, S.J., Bash, J.O., Pleim, J.E., Gan, C.M., Wong, D.C., 2018a. Long-term trends in the ambient $PM_{2.5}$- and O_3-related mortality burdens in the United States under emission reductions from 1990 to 2010. Atmos. Chem. Phys. 18, 15003–15016. https://doi.org/10.5194/acp-18-15003-2018.

Zhang, X., Zhong, J., Wang, J., Wang, Y., Liu, Y., 2018b. The interdecadal worsening of weather conditions affecting aerosol pollution in the Beijing area in relation to climate warming. Atmos. Chem. Phys. 18, 5991–5999. https://doi.org/10.5194/acp-18-5991-2018.

Zhang, Q., Zheng, Y., Tong, D., Shao, M., Wang, S., Zhang, Y., Xu, X., Wang, J., He, H., Liu, W., Ding, Y., Lei, Y., Li, J., Wang, Z., Zhang, X., Wang, Y., Cheng, J., Liu, Y., Shi, Q., Yan, L., Geng, G., Hong, C., Li, M., Liu, F., Zheng, B., Cao, J., Ding, A., Gao, J., Fu, Q., Huo, J., Liu, B., Liu, Z., Yang, F., He, K., Hao, J., 2019a. Drivers of improved $PM_{2.5}$ air quality in China from 2013 to 2017. Proc. Natl. Acad. Sci. U. S. A. 116, 24463–24469. https://doi.org/10.1073/pnas.1907956116.

Zhang, X., Xu, X., Ding, Y., Liu, Y., Zhang, H., Wang, Y., Zhong, J., 2019b. The impact of meteorological changes from 2013 to 2017 on $PM_{2.5}$ mass reduction in key regions in China. Sci. China Earth Sci. 62, 1885–1902. https://doi.org/10.1007/s11430-019-9343-3.

Zheng, Y., Xue, T., Zhang, Q., Geng, G., Tong, D., Li, X., He, K., 2017. Air quality improvements and health benefits from China's clean air action since 2013. Environ. Res. Lett. 12, 114020. https://doi.org/10.1088/1748-9326/aa8a32.

Zhu, J., Liao, H., 2016. Future ozone air quality and radiative forcing over China owing to future changes in emissions under the Representative Concentration Pathways (RCPs). J. Geophys. Res.-Atmos. 121, 1978–2001. https://doi.org/10.1002/2015jd023926.

Zhu, C., Wang, B., Qian, W., Zhang, B., 2012. Recent weakening of northern East Asian summer monsoon: a possible response to global warming. Geophys. Res. Lett. 39. https://doi.org/10.1029/2012gl051155.

Zhu, J., Chen, L., Liao, H., Dang, R., 2019. Correlations between $PM_{2.5}$ and ozone over China and associated underlying reasons. Atmosphere 10, 352. https://doi.org/10.3390/atmos10070352.